https://doi.org/10.1016/j.apenergy.2021.116607

Applicability of Indirect Evaporative Cooler for Energy Recovery in Hot and Humid Areas: Comparison with Heat Recovery Wheel

Yunran Min*, Yi Chen, Wenchao Shi, Hongxing Yang*

Renewable Energy Research Group, Research Institute for Sustainable Urban Development, The Hong Kong Polytechnic University, Hong Kong, China

Abstract

The indirect evaporative cooler (IEC), used as a novel energy recovery component for central air-conditioning (AC) systems, can cool and dehumidify the fresh air by capturing the waste thermal energy of exhaust air. To facilitate its implementation in hot and humid areas, the applicability of the hybrid AC system integrated with IEC needs to be addressed. This study quantitatively evaluated the cooling and energy-saving potentials of an IEC for energy recovery and compared it to a traditional hybrid AC system with a heat recovery wheel (HRW). On-site performance measurements were conducted in a wet market located in Hong Kong, where two air-handling units were integrated with a newly-designed IEC prototype and a commercial HRW respectively. Simulation models of the two hybrid AC systems were established based on TRNSYS platform by incorporating the numerical model of IEC and HRW respectively. The field-measurement data was used to validate the component models, and further calibrate the system models. To compare the regional adaptability of the two systems, annual simulations were conducted among 8 selected cities in southern China. Results showed that the total cooling capacities of IEC and HRW are closely related to local ambient relative humidity. Compared with the baseline AC system, the AC+IEC provides an annual energy saving intensity of 64.2–73.4 MJ/m^2 for cities with hot and moderate humid climates, which is more competitive than the AC+HRW (45.5–51.8 MJ/m^2). The annual energy saving ratios of the two types of hybrid systems range from 14.4% to 26.4%.

Keywords: Indirect evaporative cooler; energy recovery; hot-humid area; performance evaluation

Nomenclature		Greek letters	
A_{ratio}	ratio of heat transfer area to air flow volume, m^2/(m^3/s)	η_b	blower efficiency
c_p	specific heat, kJ/(kg·°C)	η_m	motor efficiency
g	gravity, m/s^2	η_{wb}	wet-bulb effectiveness
h	enthalpy of the moist air, J/kg	η_w	pump efficiency
h_{fg}	latent heat of vaporization of water, kJ/kg	ω	humidity ratio of moist air, kg/kg

* Corresponding author.
E-mail address: yunran.min@connect.polyu.hk (Y Min) and hong-xing.yang@polyu.edu.hk (H. Yang)

H_L	hydraulic head, m	ε_S	sensible effectiveness
m	mass flow rate, kg/s	ε_L	latent effectiveness
m_w	water flow rate, kg/s	φ	energy saving ratio
ΔP	fan pressure drop, Pa	λ	cooling ratio
Q	cooling capacity, kW	ξ_e	enlargement coefficient
Q_{tot}	cooling load, kW		
RH	relative humidity of moist air	Subscripts	
t	temperature, °C	a	moist air
V_r	exhaust air to fresh air ratio	C	baseline air-conditioning system
v	velocity, m/s	e	exhaust air
V	air flow volume, m^3/s	f	fresh air
W	power, kW	in	inlet of air channel
W_f	fan power, kW	out	outlet of air channel
W_m	rotary motor power, kW	p	primary air
W_p	pump power, kW	s	secondary air
		w	water

1. Introduction

For the energy use in buildings, cooling and dehumidifying fresh air constitutes 20-40% of total energy demand for the AC systems in hot and humid regions [1]. It can be a larger proportion in some public buildings with higher population density and fresh air demand [2]. Accompanied by China's accelerated urbanization process, the total floor area of large-scale public buildings has rocketed from 0.4 billion m^2 in 2008 to 1.4 billion m^2 in 2015 [3]. The soaring number of large-scale public buildings which being centrally air-conditioned has come with a huge cooling demand for fresh air and overloaded the electricity grids. Moreover, the high peak cooling load can lead to an oversized AC system, which largely increases the initial investment and results in excessive carbon emissions for the industry sector [4]. At present, the growing expectations for indoor air quality and extensive energy consumption of central AC systems have raised widespread concerns over high-efficient energy recovery technologies [5] to reduce the energy demand for fresh air handling.

The exhaust air energy recovery technology, which captures a fraction of energy from exhaust air to the supply air, can achieve remarkable energy saving in certain situations [6] [7]. Traditional heat recovery devices (i.e. air-to-air heat exchanger, enthalpy recovery wheel, desiccant wheel) have been widely used in

the central AC systems of building applications to efficiently cut down the energy demand and peak cooling load of chillers. Zhong and Kang [8] studied the applicability of the ventilators for only sensible or total heat recovery in the four climate zones of China, with the consideration of both the energy-saving and operation cost. S. H. Lee and W. L. Lee [9] evaluated the overall performance of a gas desiccant cooling system based on field measurements in a wet market located in Hong Kong, and results revealed that the annual energy cost and CO_2 emission can be reduced by 13%. Chen et al. [10] experimentally investigated the effects of process air temperature and humidity on the performance of a pre-cooling desiccant wheel. The estimated energy-saving effectiveness can guide the design of the pre-cooling desiccant wheel air-conditioning system for different climates. Liu et al. [7] studied the applicability of the enthalpy recovery wheel in five climatic zones of China by calculating the weighted coefficient of sensible heat and latent heat that dominate the enthalpy efficiency. Yamaguchi and Saito [11] developed the mathematical model for a rotary desiccant wheel and validated it by experiments under various operating conditions. It was clarified that the heat recovery desiccant cooling can be effectively hybrid with the mechanical vapour compression systems, especially for buildings with high latent loads in hot and humid areas.

Nowadays, emerging technologies for exhaust air energy recovery started to attract attention by making full use of natural and renewable energy resources to assist the mechanical vapour compression air conditioners and enhance the system's overall efficiency. Indirect evaporative cooling, as an energy-efficient and pollution-free air-cooling solution commonly used in dry climates [12], is now seeking challenges for broader application as energy recovery devices in humid subtropical areas. Some combined evaporative cooling technologies have been proposed for fresh air treatment, possessing great potentials to generate comfortable conditions [13]. Karami et al. [14] numerically investigated the performance of an indirect evaporative cooler (IEC) in a solar desiccant AC system for buildings in Bandar Abbas. Based on the simulations, the IEC unit integrated into the desiccant AC system can significantly reduce the sensible cooling load and satisfy the thermal comfort conditions. Lin et al. [15] studied the performance of combined dehumidification and evaporative cooling system by an experimentally-validated computational model. The cooling performance of a new cross-flow dew point IEC prototype proposed in Ref. [16] degrades under humid weather conditions, while the air dehumidification process proposed prior to the IEC can improve the energy efficiency by 70-135%. Zanchini and Naldi [17] presented the energy-saving obtainable by coupling an M-cycle IEC to the conventional AC system in an office building. The dynamic simulation results showed that using IEC to cool the recirculated air for a coupled heat recovery system can offer 37.6% of energy savings during July and August in Milan. Cui et al. [18] developed a practical modified LMTD method suitable for designing and analyzing the IEC heat exchangers. Through theoretical study, the IEC

unit coupled with the central AC system can handle 35-47% of the fresh air cooling load in tropical climate by employing the room return air as working fluid [19].

The integration of the traditional heat recovery wheel (HRW) with the refrigeration cycle has already gained widespread acceptance with commercially available devices on the existing AC markets [20]. However, as the leakage ratio of rotary wheel is about 5% of the design volume [21], the cross-contamination from the return air to the supply air side remains a danger for long-term operation, especially in buildings that require strict indoor pollutant control. To guarantee public health and also meet the ventilation requirement, novel energy recovery devices with entirely separate inner channels has gained increasing attention, such as indirect evaporating cooling [22]. Currently, the research on the IEC hybrid AC systems for exhaust air energy recovery is mainly based on numerical studies and laboratory tests [23]. The gaps between the theoretical research and its implementation in hot and humid areas mainly include: 1) much less reporting on the field-based application of IEC with dehumidification effect; 2) the applicability of IEC to be used as an energy recovery device in different areas remains unexplored; 3) the energy performance assessment of IEC and its comparisons with traditional energy recovery devices such as HRW have rarely be addressed.

These issues motivated the present work to incorporate an on-site measurement and investigate the applicability between the indirect evaporative cooler (IEC) and the traditional heat recovery wheel (HRW) for exhaust air energy recovery in hot and humid regions. First, an IEC prototype was designed, fabricated and installed in parallel with an HRW unit in a wet market located in Hong Kong. Based on the operation data, the cooling availability of the two systems was illustrated and compared in terms of both sensible cooling and dehumidifying performance. Besides, the developed numerical models of the IEC and HRW for predicting the outlet air conditions were validated using the field-measurement data. By incorporating the models of energy recovery components, the simulation models of the two hybrid AC systems were established in TRNSYS platform, respectively. At last, the regional adaptability of the two systems on both cooling and energy-saving potentials were addressed among 8 cities in southern China through the annual simulations. This work provides an extensive performance comparison between the two types of hybrid fresh air-handling technologies, contributing to the implementation of efficient central AC systems for energy recovery in hot and humid regions.

2 Indirect Evaporative Cooler (IEC) for exhaust air energy recovery in hot and humid areas

In recent years, a novel central AC system coupled with indirect evaporative cooler (AC+IEC) [24] was proposed, which can precool the fresh air by capturing the cooling potential of exhaust air from indoor space. The system diagram is shown in Fig. 1. In the IEC, a large wet-bulb depression of the secondary air

can be achieved by using the exhaust air to evaporate the water in the wet channels, which facilitates the primary air cooling process in the dry channels. The circulated spraying water can be evaporated gradually and emitted with the exhaust air. A constant pressure water supplement device should be provided in IEC to supply make-up water for the spraying system. In hot and humid areas, the IEC can achieve both sensible and latent heat recovery because of possible condensation deriving from highly humid fresh air [25]. Compared to the traditional HRW system, the IEC owns advantages as a lower pressure drop [26], free from the periodic replacement of desiccant materials, and free from cross-contamination due to the separate channels. There is a great potential for IEC as an alternative exhaust air energy recovery technique applied in hot and humid areas, while its energy saving potential needs to be further investigated.

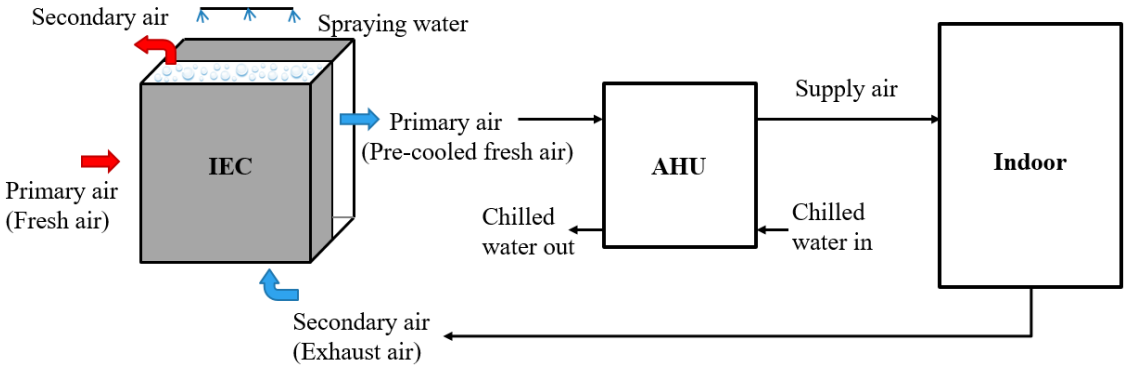

Fig. 1 System diagram of AC+IEC.

3 On-site measurement

In this study, the cooling availability of two hybrid fresh air-handling systems (i.e. AC+IEC, AC+HRW) for exhaust air energy recovery was estimated through an on-site measurement of a practical engineering project. The project was conducted in a wet market in Hong Kong. The wet market, which requires a high fresh air volume and concentrated disposal of exhaust air, was selected as the typical building for exploring the applicability analysis of hybrid fresh air-handling systems. Hong Kong has a typical hot and humid climate with the annual monthly mean temperature varies between 15–32 °C and the relative humidity varies between 69–83% [27]. The cooling load exists all year round, which results in excessive energy use for air-conditioning.

3.1 Test overview

The wet market building is employed to sells fresh meat, seafood and live animals including poultry. To avoid the diffusion of smells and contaminants, the wet market building requires a high ventilation rate and a larger exhaust air volume than the fresh air volume to keep a negative pressure in the market. As the

return air is rejected to ambient without recirculation, the 100% fresh air AC system is adopted to handle both the sensible and latent cooling load over the whole year. Fig. 2 shows the view of the plant room in the served wet market. The building information and system characteristics of the wet market are summarized in Table 1. In this wet market, the condensate water of mechanical cooling can be collected and then serves as make-up water for the IEC spraying system. Simultaneous usage of AC condensate water and IEC spray water can be self-sufficient.

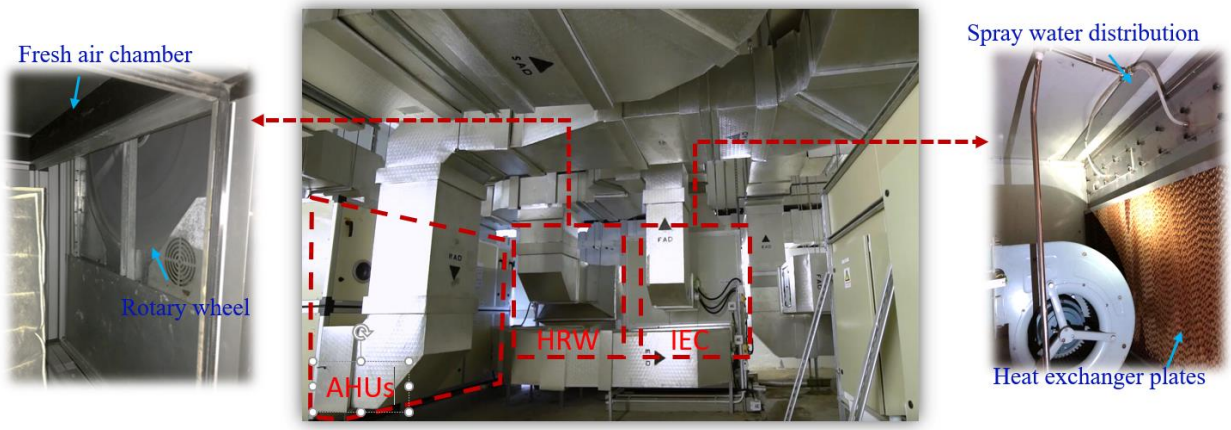

Fig.2 The view of plant room for central AC system

Table 1 Summary of building information and system characteristics

Description	Details
Building information	
Building area (m^2)	260
Floor number	2
Window-to-wall ratio	0.2
Glass characteristics	10 mm clear glass
U-value of external wall ($W/m^2 \cdot °C$)	1.5
Lighting load (W/m^2)	22.2
Electrical equipment load (W/m^2)	40
Occupancy	60
Evaporation rate of wet sources (kg/h)	32.5
System characteristics	
AC set point	24°C, 65%
AC operation duration	6:00 - 20:00
Ventilation rate (ACH)	7
Number of AHU units	2
Rated cooling capacity (kW)	121
Heat rejection method of chillers	air-cooled
Measured EER_c	1.9
Fresh air flow rate (m^3/h)	6228
Exhaust air flow rate (m^3/h)	6840

Heat recovery wheel	
Rotor type	enthalpy
Wheel dimensions (L×W×H in m)	1.33×0.34×1.33
desiccant material	silica gel
Wheel speed	10 rpm
Motor power (kW)	0.18
Pressure drop (Pa)	180
Face velocity (m/s)	3.1
Indirect evaporative cooler	
Number of channel pairs	100
Channel gap (mm)	4
Heat exchanger plate (m×m)	1×1
Primary air pressure drop (Pa)	32
Secondary air pressure drop (Pa)	96
Circulating water flow rate (kg/s)	3.31

In this wet market, the intake fresh air is processed by two sets of the same AHUs that are coupled to an indirect evaporative cooler (IEC) and a rotary wheel (HRW) respectively. The HRW unit was selected from compatible mature products in the market, while the IEC prototype for exhaust air energy recovery was fabricated by a manufacturer based on our provided design parameters from the previous optimization study [28]. The detailed design parameters are as shown in Table 1. The two plants share a similar NTU number of 3.6, which allows further comparisons on cooling and energy-saving performance. Fig. 2 also presents the internal configurations of the two fresh air pre-handling units. These two trial systems operate simultaneously under the operation scheme shown in Fig. 3, with one for IEC standby and another for HRW standby. The test parameters and sensors of the central AC system in the wet market are listed in Table 2. The setting of the time interval for the measurement is 1 minute. Real-time test data are transmitted to a deployed remote monitoring system which enables the view of current sensor values, remote control and retrieves of data sources, as shown in Fig. 4.

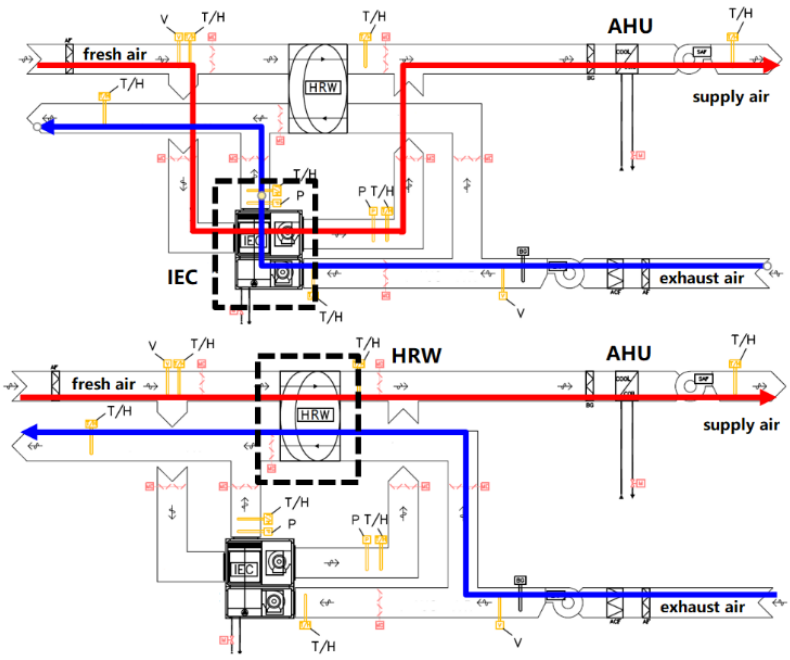

Fig. 3 Schematic diagram of the two sets of trial systems

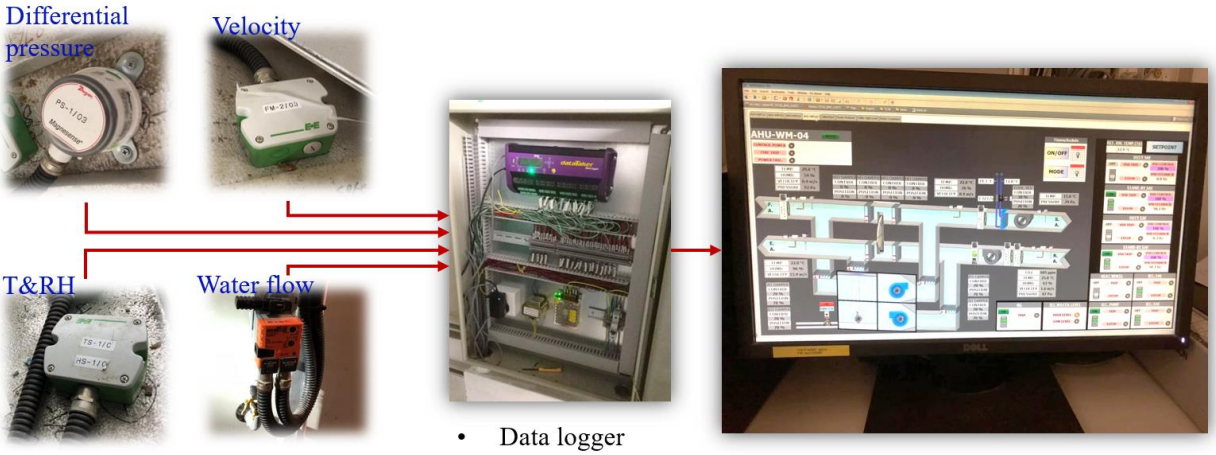

Fig.4 Configuration of the monitoring system

Table 2 Test parameters and sensors

Parameter	Range	Accuracy	Supplier
Temperature, Humidity	-15–60℃ 10–95% RH	±0.3℃ ±2.5% RH	E+E Co., Pt1000, Model: EE160
Air velocity	0–10 m/s	±0.2m/s	E+E Co., Model: EE65
Pressure drop	< 250, 500, 1250 Pa	±1%	Dwyer Co., Model: MS-112
Water flow rate	0.36–34.2 gpm	±2%	Belimo Co., Model: FM125
Data logger	Dadataker, Model: DT80, 12 channels		

3.2 Test results

Two types of hybrid fresh air handling systems were implemented in the selected wet market for long-term operation. For the proposed IEC heat exchanger, the sensitivity analysis conducted in our previous study [28] has indicated that both the humidity of fresh air and exhaust air can greatly influence the sensible heat transfer of IEC, while the latent heat transfer is mainly decided by the temperature and humidity of fresh air. In the present study, the IEC serves as an energy recovery unit in the AC system, and the exhaust air from conditioned space works as the secondary air with relatively stable temperature and humidity (24°C, 65%). Therefore, the most influential operation parameters of the proposed IEC in the hybrid AC system are selected as the inlet fresh air temperature and humidity. The test results during a typical day in the cooling season were selected to compare the temperature and humidity variation of the processed air from IEC and HRW. On this day, the average outdoor temperature and relative humidity during the operation period were 28.3°C and 83%, respectively. The test results are as shown in Fig. 5, and the gray areas represent the operation hours of the AC system. The space-filling of corresponding curves indicates the 95% uncertainty bands.

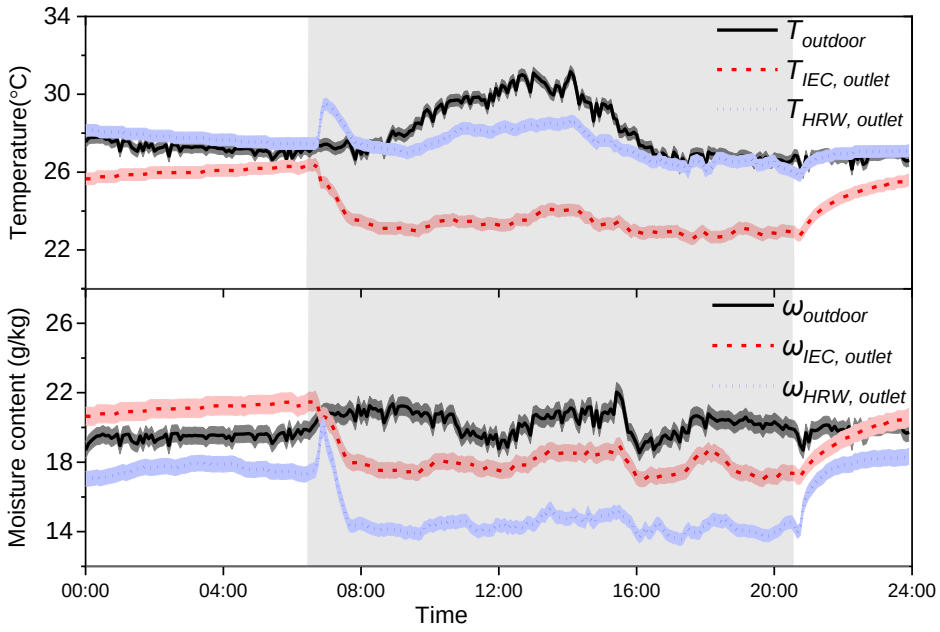

Fig. 5 Temperature and humidity variation of the supply air from IEC and HRW in a typical day

By utilizing the water evaporation, the IEC was able to cool the air from 31.2°C down to maintain at 24.0°C with a relatively stable condensed moisture of 2.5 g/kg. However, the performance of HRW was more sensitive to the exhaust air states, as the outlet temperature and humidity of fresh air fluctuate before the

indoor space was conditioned to the setting values. The outlet air temperature of HRW was 4.0°C higher than that of IEC on average, while the average outlet air humidity ratio of HRW was 3.2g/kg lower than that of IEC. Therefore, the two systems demonstrated different preferences in terms of sensible cooling and dehumidifying effect, indicating that a comprehensive comparison should be conducted to evaluate their performances in total heat recovery and energy-saving potential.

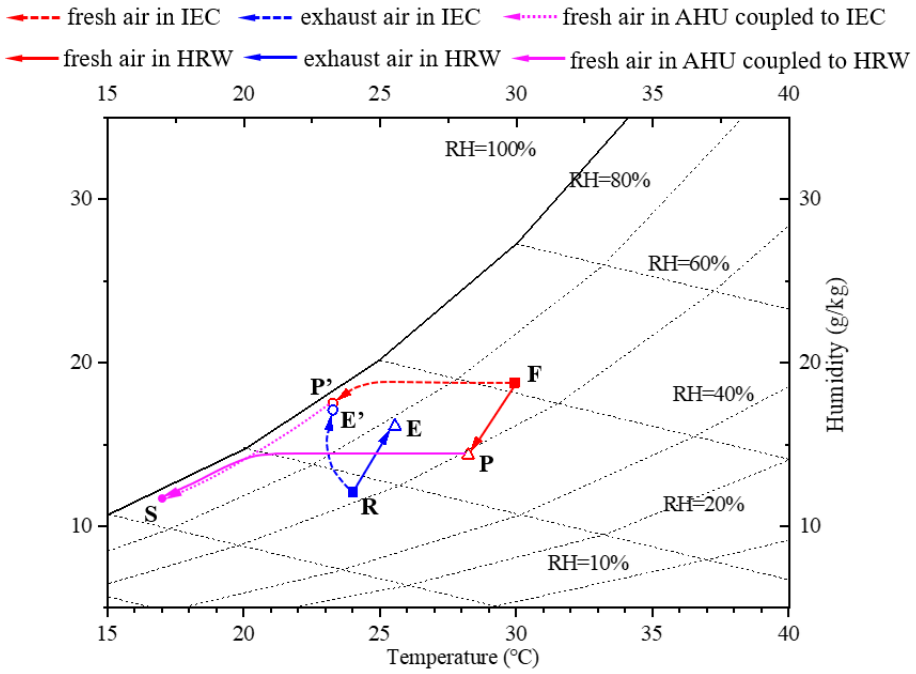

Fig. 6 Air-handling process of the AC+IEC and AC+HRW

Fig. 6 illustrates the air handling processes of IEC and HRW at 12:00 of this typical day in a psychrometric chart. In the fresh air chamber of rotary wheel, the temperature and equilibrium enthalpy of the desiccant are all lower than those of the fresh air, so the fresh air is cooled and dehumidified from point F to point P. Excess heat and moisture are transferred to exhaust air (from point R to point E) when the rotary wheel turns back to the exhaust air side. However, the IEC differs from the HRW in terms of the heat and mass transfer mechanisms. Driven by the enthalpy potential of water vaporization, the fresh air in IEC is sensibly cooled to approach its dew point temperature, and is dehumidified to point P' owing to the condensation effect. The return air evaporates the spraying water and changes from state R to state E', taking away the heat and moisture to the outdoor atmosphere. The cooling capacity of the HRW unit (Q_{HRW}) or IEC unit (Q_{IEC}), and the cooling load of AHU coupled to HRW (Q_{AHU_w}) or IEC (Q_{AHU_i}) were calculated by Eqs. (1) - (4). According to the measured data at 12:00, the HRW and IEC handled 28.1% and 31.5% of fresh air cooling load for the central AC system, respectively.

$$Q_{HRW} = m \cdot (h_F - h_P) \quad (1)$$

$$Q_{AHU_w} = m \cdot (h_P - h_S) \quad (2)$$

$$Q_{IEC} = m \cdot (h_F - h_{P'}) \quad (3)$$

$$Q_{AHU_i} = m \cdot (h_{P'} - h_S) \quad (4)$$

where m is the air flow rate, kg/s; h_F is the enthalpy values of the outdoor air, J/kg; h_P and $h_{P'}$ are the enthalpy values of the processed air from HRW and IEC respectively, J/kg; h_S is the enthalpy value of the supply air from AHU, J/kg.

4. Models of IEC and HRW

4.1 Heat recovery wheel (HRW)

In the HRW, the desiccant materials are embedded in a rotary wheel with small channels that rotates continuously between the fresh air and exhaust air chambers. The heat and moistures extracted from fresh air can be taken away by the return air as the wheel turns. A mathematical model for the coupled heat and mass transfer in an HRW was established by considering the two-dimensional heat conduction and dual-transient diffusion in both the axial (x) and radial (z) direction. This model is transient, and the converged values are required for each time step (t). Due to the symmetry of each flow channel, a half-size channel is used as a single grid. Based on energy conservation and mass balance, the governing equations of the air stream and desiccant are as follows. The details of assumptions made in the model and the normalization of equations are presented in Ref. [29] [30].

For the heat and mass balance of the air stream:

$$\frac{1}{u_a}\frac{\partial T_a}{\partial t} + \frac{\partial T_a}{\partial x} = \frac{4h}{\rho_a u_a d_e c_{pa}}(T_s - T_a) \quad (5)$$

$$\frac{1}{u_a}\frac{\partial \omega_a}{\partial t} + \frac{\partial \omega_a}{\partial x} = \frac{4h_m}{\rho_a u_a d_e}(\omega_s - \omega_a) \quad (6)$$

where, h and h_m are the convective heat transfer coefficient and the mass transfer coefficient between the air stream and solid surface, respectively, W/(m^2·K) and kg/(m^2·s); d_e is the hydrodynamic diameter of the channel, m; the subscripts ‘s’ and ‘a’ refer to ‘wall surface’ and ‘air’ respectively.

For the heat and mass balance in the desiccants:

$$\rho_d c_{tot}\frac{\partial T_d}{\partial t} = \lambda_d\left(\frac{\partial^2 T_d}{\partial x^2} + \frac{\partial^2 T_d}{\partial z^2}\right) + q_{st}\rho_d\frac{\partial w}{\partial t} \quad (7)$$

$$\varepsilon_t\rho_a\frac{\partial \omega}{\partial t} + \rho_d\frac{\partial w}{\partial t} = \rho_a\left[\frac{\partial}{\partial x}\left(D_A\frac{\partial \omega}{\partial x}\right) + \frac{\partial}{\partial z}\left(D_A\frac{\partial \omega}{\partial z}\right)\right] + \rho_d\left[\frac{\partial}{\partial x}\left(D_S\frac{\partial w}{\partial x}\right) + \frac{\partial}{\partial z}\left(D_S\frac{\partial w}{\partial z}\right)\right] \quad (8)$$

where, ρ_d and λ_d are the density and thermal conductivity of the adsorbent wall, respectively, kg/m^3 and W/(m·K); T_d is the temperature of the desiccant; K; q_{st} is the adsorption heat of the desiccants, J/kg; ε_t is the porosity of the desiccant; c_{tot} is the total specific heat capacity of the wet desiccant wall, J/kg·K; ω and w are the moisture contents of air and desiccant, respectively, kg/kg; D_A is the gas diffusion; D_S is the surface diffusion. The calculation for these base properties and parameters used in the HRW model are summarized in Appendix A.

Before being numerically solved by the finite difference method, the equations were discretized into each grid which is divided by nodal points. The numbers of nodes are 30 in axial, 10 in thickness, and 60 in time. For each time interval, the temperature and humidity fields in the air stream were derived to integrate the mean outlet values. The model was validated by experiments under typical summer operating conditions with the bias differences within 3.7% for outlet air temperature and 5.21% for outlet air humidity [29].

4.2 Indirect evaporative cooler (IEC)

Concerning the condensation of fresh air that sometimes occurs and therefore influences the total heat transfer, the model of IEC should take into account the operating states with and without dehumidification. A 2-D numerical model for cross-flow IEC developed by previous works can be used to predict the cooling and dehumidifying performance under a wide range of operating conditions. A single channel pair of primary air and secondary air was used as the control volume to establish the governing equations as follows. The details of assumptions and simplification made in the model are presented in Ref. [28, 31].

For energy and mass balance in the secondary air channel:

$$h_s(t_w - t_s) \cdot dxdy + h_{fg} h_{ms}\left(\omega_{t_w} - \omega_s\right)\sigma \cdot dxdy = \dot{m}_s \frac{\partial i_s}{\partial y} \cdot dy \tag{9}$$

$$h_{ms}\left(\omega_{t_w} - \omega_s\right)\sigma \cdot dxdy = \dot{m}_s \frac{\partial \omega_s}{\partial y} \cdot dy = \frac{\partial m_e}{\partial y} \cdot dy \tag{10}$$

where, h_s and h_{ms} are the heat and mass transfer coefficients between secondary air and plate surface, respectively, W/(m^2·°C) and kg/(m^2·s); h_{fg} is the latent heat of vaporization of water, kJ/kg; σ is the surface wettability; ω_{t_w} is the moisture content of saturated air at the plate surface temperature, kg/kg.

For the primary air in the grid element under non-condensation states ($t_{dew,p} < t_w$), the energy balance can be derived in Eq. (11). When the primary air condensation occurs, i.e., $t_{dew,p} > t_w$, a new set of governing equation should be established to represent the mass balance in primary air channel, as shown in Eq. (12):

$$h_p\left(t_p - t_w\right) \cdot dxdy = c_{pa} \dot{m}_p \frac{\partial t_p}{\partial x} \cdot dx \tag{11}$$

$$h_{mp}\left(\omega_{t_w}-\omega_p\right)\cdot dxdy=\dot{m}_p\frac{\partial\omega_p}{\partial x}\cdot dx=-\frac{\partial m_c}{\partial y} \tag{12}$$

where, $t_{dew,p}$ is the dew point temperature of primary air, ℃; h_p and h_{mp} are the heat and mass transfer coefficients between primary air and plate surface, respectively, W/(m^2·℃) and kg/(m^2·s).

For the heat exchanger plate between the two channels, the energy balance under non-condensation states can be derived in Eqs. (13). When the condensation occurs, Eq. (13) will be replaced by Eq. (14):

$$\dot{m}_s\frac{\partial i_s}{\partial y}-c_{pa}\dot{m}_p\frac{\partial t_p}{\partial x}=\ c_{pw}t_{ew}\frac{\partial m_e}{\partial y} \tag{13}$$

$$\dot{m}_s\frac{\partial i_s}{\partial y}-\dot{m}_p\frac{\partial i_p}{\partial x}=\ c_{pw}t_{ew}\frac{\partial m_e}{\partial y}+c_{pw}t_{cw}\frac{\partial m_c}{\partial y} \tag{14}$$

where, the subscripts ‘s’, ‘p’, ‘w’, ‘e’ and ‘c’ refer to ‘secondary air’, ‘primary air’, ‘heat exchanger plate’, ‘evaporative water film’ and ‘condensate water film’, respectively.

The boundary conditions and the operating parameters used in the IEC model were given in Appendix A. Using the finite difference method, the partial differential equations for each element were discretized into algebraic equations and then solved by the iteration process. The grid size 100×100 was selected to achieve minimum computation time within the given tolerance of accuracy. The numeral model of IEC has been validated by the experiments under both operating conditions with or without condensation [28]. Good agreement can be found between the simulation and experimental results with the discrepancies of 5.9% for outlet air temperature and 2.4% for outlet air humidity.

4.3 Model validation

The field-measurement data of the wet market were used to validate the numerical models of IEC and HRW. The averaged values of measured fresh air inlet temperature and relative humidity in a 5-min interval were collected as inputs for the models to derive the temperature and relative humidity at the outlet. The predicted data for sensible and latent cooling capacity were compared to the measured data calculated by the test values of inlet and outlet temperature and relative humidity in a 1-min interval. Fig. 7 compares the actual and predicted cooling capacity of IEC and HRW at 5-min intervals on average during a typical day. The randomness of measured and predicted data for sensible and latent loads can result from the dynamic variations of outdoor air states, nonuniform air stream in the duct and the thermal capacity of indoor air. The measurement uncertainty on the Q_{sen} and Q_{lat} were estimated as 9.4% and 12.7%, respectively. It is found that the mean absolute relative difference (MARD) is 5.2% between the predicted and actual sensible cooling capacity of HRW, and is 6.7% between the predicted and actual sensible cooling capacity of IEC. The MARD between the predicted and actual latent cooling capacity of HRW is 8.6%. For the latent cooling

capacity of IEC, the MARD between the predicted and actual values is 9.3%. The accuracy levels of IEC and HRW models are considered acceptable to be used in the simulation platforms.

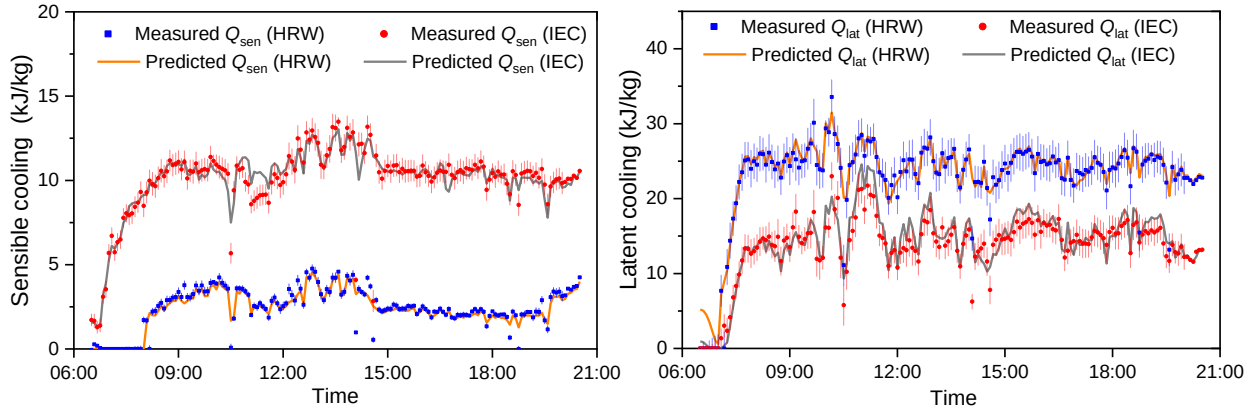

(a) sensible cooling capacity (Q_{sen}) (b) latent cooling capacity (Q_{lat})

Fig. 7 Validation of the IEC and HRW models

5. Simulation platform for regional applicability analyses

In China, the hot and humid regions are defined by climatic indicators that have an average temperature greater than 10°C in January and 25°C–29°C in July [32]. According to the meteorological data [33], 8 typical cities with hot and humid climates were selected in southern China. The tested wet market is selected as an objective for setting up the building model applied in these cities. Annual simulations of 8790 hours were conducted in all the selected cities. As the wet market building is an extremely damp place where people gathered, the building cooling load exists all-year-round under the hot and humid climate. The heating is not considered in the wet market buildings because of the very limited demand for short periods. The summer climatic design conditions of these cities are summarized in Table 3 by referring to the ASHRAE Handbook of Fundamentals [34]. The design conditions based on dry-bulb temperature (DBT), wet-bulb temperature (WBT) and dew point (DPT) are directly related to the extremes of sensible, enthalpy and moisture loads of the outdoor air, respectively.

Table 3 Cooling and evaporation design conditions for the 8 selected cities

Index	City	Cooling DBT/CWBT (°C)	Evaporation WBT/CDBT (°C)	Dehumidification DP/CDBT (°C)
1	Haikou	35.1 / 26.8	28.0 / 32.5	26.9 / 30.0
2	Shantou	34.2 / 27.1	28.6 / 31.8	28.0 / 30.6
3	Hong Kong	34.0 / 26.5	27.7 / 31.1	26.9 / 30.2
4	Nanning	35.0 / 26.2	27.7 / 31.9	26.7 / 29.7

5	Guangzhou	35.9 / 26.2	27.7 / 31.7	26.9 / 29.6
6	Fuzhou	35.6 / 26.7	27.7 / 33.2	26.2 / 30.7
7	Changsha	36.4 / 26.1	27.8 / 32.9	26.6 / 30.5
8	Wenzhou	33.9 / 27.3	28.0 / 32.6	26.8 / 30.5

* These design conditions are corresponding to 0.4% annual cumulative frequency of occurrence.

5.1 The system model

A dynamic platform was built to evaluate and compare the regional adaptability of the two exhaust air energy recovery systems by using TRNSYS [35]. Thermal properties of the building envelope and the indoor properties (shown in Table 1) were input for simulation. Typical meteorological year (TMY) data of the 8 cities were introduced for the building load simulation. The HRW and IEC components were created using new types for linking the Matlab code to TRNSYS simulation program. Details of the HRW and IEC models are explained in section 4. Based on the input states of fresh air and exhaust air, the temperature and humidity ratio of the processed air leaving from IEC or HRW unit ($t_{ahu,in}$, $\omega_{ahu,in}$) were calculated and outputted to the AHU.

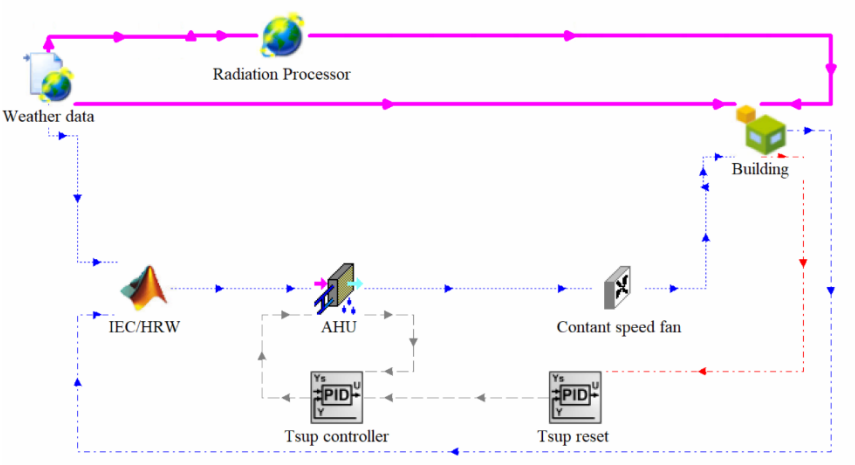

(a) Scenario A: without indoor humidity control

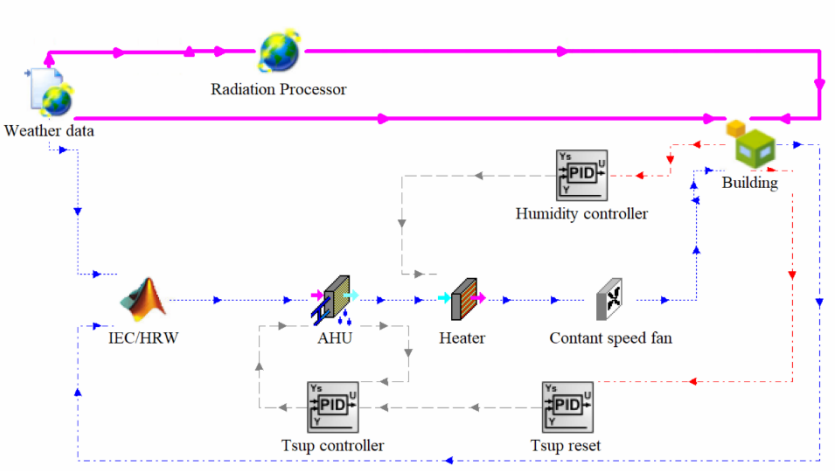

(b) Scenario B: with indoor humidity control

Fig. 8 Framework of the simulation model

The system model can be established with the framework demonstrated in Fig. 8. In this study, the simulations were conducted by considering two scenarios with or without indoor humidity control, as the conventional AC system for commercial and residential applications only controls the room temperature [36]. Indoor humidity control is needed in spaces requiring high-quality thermal comfort or industrial buildings [37]. Under scenario A, only the room temperature is maintained at the set-point, and the moisture is extracted from the supply air coincidentally. Under scenario B (with indoor humidity control), the desired room humidity ratio is achieved by the overcooling that needs to be offset through a reheating process. After pre-cooled by the IEC or HRW, the fresh air enters the AHU and further be treated to the set-point. The cooling coil valve in AHU is modulated by a PID controller to maintain the supply air temperature at the corresponding set-point. The indoor air relative humidity is controlled by a PID controller below a preset threshold by modulating the AHU heating coil valve. For the purpose of dehumidification, the supply air is overcooled by the cooling coil and then reheated by the heating coil to reach the predefined supply air temperature set-point.

Operation strategies of the two AC systems with different fresh air pre-handling units were set as shown in Table 4. The operation period of the two types of hybrid AC system is from 6:00 to 20:00. The two systems are turned on only if the indoor air temperature is higher than the set-point, otherwise, they are turned off with the fresh air and exhaust air be bypassed and sent to indoor or outdoor spaces directly. The two energy recovery components are employed using on-off control. The air fans in IEC or HRW operate under the rated flow rates which are designed to meet the required ventilation rate of the wet market. During the cooling season, the HRW works only if the fresh air temperature ($t_{f,in}$) is higher than the exhaust air

temperature ($t_{e,in}$), so as to avoid heating the fresh air and causing additional electricity consumption. For the IEC, when the inlet temperature of fresh air is lower than the wet-bulb temperature of exhaust air ($t_{e,in}$), it stops running and the fresh air is bypassed and supplied directly into the AHU. The flow rate of chilled water that goes through the cooling coil of AHU was modulated by local controllers to cool and dehumidify the supply air to a level (t_{supset}) for satisfying the indoor thermal comfort.

Table 4 Operation strategies of the AC systems in the wet market

No.	System type	Unit	Schedule/condition
1	HRW+AHU	AHU	On: 6:00-20:00, $t_{supset} \leq t_{ahu,in}$ Off: others
		HRW	On: 6:00-20:00, $t_{e,in} \leq t_{f,in}$, $t_{supset} \leq t_{f,in}$ Off: others
2	IEC+AHU	AHU	On: 6:00-20:00, $t_{supset} \leq t_{ahu,in}$ Off: 20:00-6:00
		IEC	On: 6:00-20:00, $t_{wb,e} \leq t_{f,in}$, $t_{supset} \leq t_{f,in}$ Off: others

5.2 Performance indexes

To compare the cooling potentials of the two fresh air pre-handling systems operated in different regions of southern China, the cooling ratio (λ) is proposed in Eqs. (15)-(16). It was defined as a ratio of the cumulated cooling capacity of the fresh air pre-handling unit (IEC or HRW) to the cumulated total cooling load of the AC system.

$$\lambda_{HRW} = \frac{\sum_{\tau=s}^{\tau=e} Q_{HRW}}{\sum_{\tau=s}^{\tau=e} Q_{tot}} \times 100\% \quad (15)$$

$$\lambda_{IEC} = \frac{\sum_{\tau=s}^{\tau=e} Q_{IEC}}{\sum_{\tau=s}^{\tau=e} Q_{tot}} \times 100\% \quad (16)$$

where, s and e represent the start and end times for cooling, respectively.

The energy consumption of the AC system with different exhaust air energy recovery technologies includes the additional power of the selected pre-handling system (W_{HRW} or W_{IEC}), and the electricity use of chillers (W_C) for further conventional cooling and dehumidification of the fresh air. For the HRW unit, the energy demand includes the power of the rotary motor (W_m), fresh air fan power ($W_{f,1}$) and exhaust air fan power ($W_{f,2}$), as expressed in Eq. (17).

$$W_{HRW} = W_m + W_{f,1} + W_{f,2} \quad (17)$$

where W_m varies with the rotation speed which is related to the wheel thickness. For a desiccant wheel with 0.4m thickness, the rotation speed has to be lower than 10 rpm for minimizing cross-contamination [21]. In the studied wet market, the rated motor power of HRW is 0.18kW with a rotation speed of 10 rpm.

Consisting of multiple alternative dry and wet channels, the IEC makes use of water evaporation for cooling purposes by running only a small pump and fans. The power-consuming components in an IEC unit include a primary air fan ($W_{f,p}$), a secondary air fan ($W_{f,s}$), and a circulation water pump (W_p), as shown in Eq. (18).

$$W_{IEC} = W_p + W_{f,p} + W_{f,s} \tag{18}$$

The fan power W_f of IEC or HRW depends on the pressure drop through the heat exchanger, and can be calculated using Eq. (19). Previous literature pointed out that the pressure drop in IEC (20–120Pa) [38] is much lower than that in the desiccant wheel (around 200 Pa) [39]. In this study, the pressure drops of the two pre-cooling units were tested, and the averaged values were listed in Table 1.

$$W_f = \frac{V \cdot \Delta P}{\eta_b \eta_m} \tag{19}$$

where V is the air flow volume, m^3/s; ΔP is the fan pressure drop caused by the heat exchanger of IEC or HRW, Pa; η_b is the blower efficiency, 0.7; η_m is the motor efficiency, 0.9.

The power of the pump (W_p) in the IEC can be calculated using Eq. (20).

$$W_p = \frac{m_w \cdot g \cdot H_L}{\eta_w} \tag{20}$$

where, m_w is the mass flow rate of circulating water, kg/s; H_L is the water circulating resistance, which is designed to be 19.5m by considering the head loss of gravity, spray nozzle and valve; η_w is the pump efficiency, 0.85.

The total energy consumption of the AC system coupled with different fresh air pre-handling units, E_{AC+HRW} and E_{AC+IEC} respectively, are calculated using Eqs. (21) and (22).

$$E_{AC+HRW} = \frac{\sum_{\tau=s}^{\tau=e}(Q_{tot} - Q_{HRW})}{EER_C} + \sum_{\tau=s}^{\tau=e} W_{HRW} \tag{21}$$

$$E_{AC+IEC} = \frac{\sum_{\tau=s}^{\tau=e}(Q_{tot} - Q_{IEC})}{EER_C} + \sum_{\tau=s}^{\tau=e} W_{IEC} \tag{22}$$

where, EER_C is the cooling energy efficiency ratio of the conventional AC system, assumed to be 3.5 according to the common products in the Chinese market [40]. For the simulation scenario with the indoor

humidity control, the energy consumption of the heater should also be considered, and the Eqs. (21)-(22) were substituted by the Eqs. (23)-(24).

$$E_{AC+HRW} = \frac{\sum_{\tau=s}^{\tau=e}(Q_{tot} - Q_{HRW})}{EER_C} + \sum_{\tau=s}^{\tau=e} W_{HRW} + \sum_{\tau=s}^{\tau=e} W_{reheat} \quad (23)$$

$$E_{AC+IEC} = \frac{\sum_{\tau=s}^{\tau=e}(Q_{tot} - Q_{IEC})}{EER_C} + \sum_{\tau=s}^{\tau=e} W_{IEC} + \sum_{\tau=s}^{\tau=e} W_{reheat} \quad (24)$$

where W_{reheat} is the power demand during the reheating process, kJ. In this study, a small heat pump is assumed for providing reheating with a COP of 3.5.

To evaluate the energy efficiency of the IEC and HRW for fresh air pre-handling in hot and humid regions, the energy-saving ratio is defined for each of the two systems by comparing to the energy consumption of the baseline AC system without exhaust air energy recovery unit (E_C), as expressed in Eqs. (25)-(27).

$$E_C = \frac{\sum_{\tau=s}^{\tau=e} Q_{tot}}{EER_C} \sum_{\tau=s}^{\tau=e} W_{reheat} \quad (25)$$

$$\varphi_{HRW} = \frac{E_C - E_{AC+HRW}}{E_C} \times 100\% \quad (26)$$

$$\varphi_{IEC} = \frac{E_C - E_{AC+IEC}}{E_C} \times 100\% \quad (27)$$

5.3 System calibration

The calibration is accomplished by comparing the simulation results with the measured data from the wet market. The variables used for calibration include the cooling capacity of IEC and HRW, both from the simulations and the field-based measurement in Hong Kong. To obtain a valid calibration, the weather data, operation schedule and system characteristics from the installation were collected as detailed input data for simulations. Fig. 9 shows the actual and simulated monthly cumulative cooling capacity of IEC and HRW in the wet market. The results show consistency in the variation trends throughout the year, in which the HRW has higher cooling capacity in the summer season (Jun., Jul., Aug.), whereas the IEC achieves more heat recovery during transition seasons (Mar., Apr., Oct., Nov.). Based on the measured data of the wet market, the annual cumulative cooling capacity of HRW (233 kWh/m^2) is slightly (6%) higher than that of IEC (220 kWh/m^2). Two statistical indices were used to assess the calibration of the system models: the mean bias error (MBE) and the coefficient of variation of the root mean squared error (CVRMSE). The simulation results of IEC indicate an MBE value of 2.8% and a CVRMSE value of 12.2%. The simulation results of HRW indicates an MBE value of 3.4% and a CVRMSE value of 15.4%. These calibration results can meet the criteria of ASHRAE Guideline 14 [41] on a monthly-based data sampling period, so the developed model can be considered as validated.

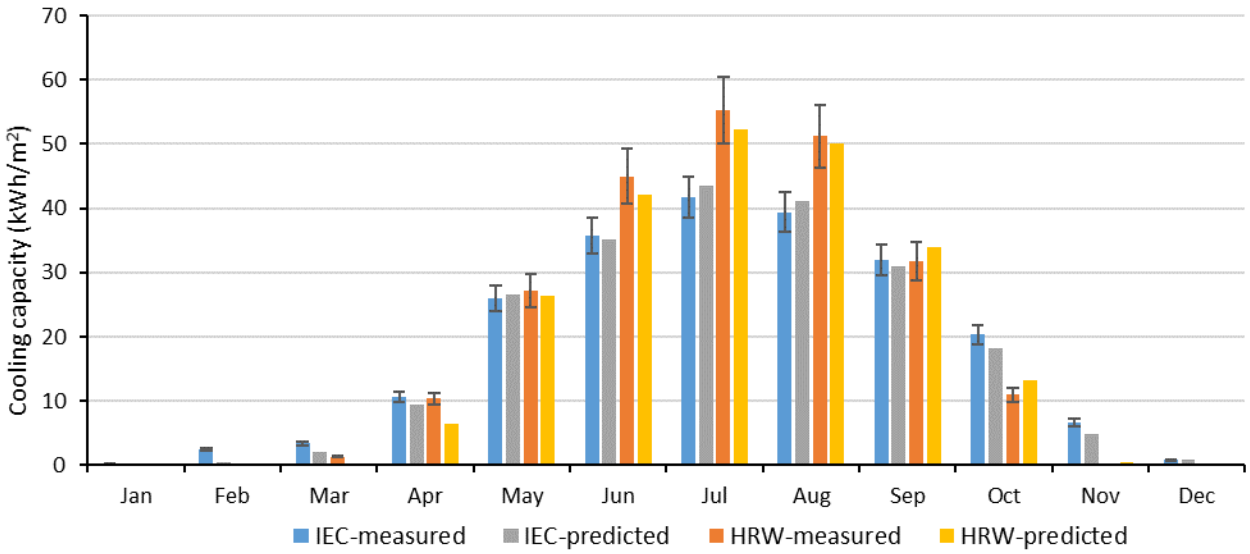

Fig. 9. The measured and simulated monthly cumulative cooling capacity of IEC and HRW in Hong Kong

6. Results and discussion

Based on the developed simulation platform, the cooling performance, as well as energy-saving potentials of the two types of hybrid fresh air-handling systems (i.e. AC+IEC and AC+HRW) were investigated. The cooling load handled by IEC and HRW respectively during the cooling season were simulated in 8 selected cities. The peak cooling load reduction was compared between the two systems. Besides, two scenarios were considered to analyze the effect of indoor humidity control on the energy recovery efficiency for processing the fresh air. Apart from that, the differences between the total cooling capacity of IEC and HRW were correlated with the local ambient relative humidity. Finally, the energy-saving ratios and regional applicability of the two systems were analyzed in the selected cities.

6.1 Peak load reduction

Fig. 10 shows the profiles of the cooling load handled by IEC and HRW respectively in the 8 selected cities. The annual cumulated building cooling load for different cities varied from the highest of 669.4 MWh in Haikou (shown in Fig. 10a) to the lowest of 381.4 MWh in Wenzhou (shown in Fig. 10h). It can be seen that cooling is required almost all year due to the hot and humid climate for these cities. The HRW provides a higher cooling capacity than the IEC during most of the summertime. However, for other seasons with a moderate humidity ratio, the HRW hardly operates since it is not capable of providing cooling or dehumidification. By contrast, the IEC is feasible for longer operation periods throughout the year, as it also handles parts of the indoor cooling load during the transition seasons by utilizing the enthalpy potential of water evaporation.

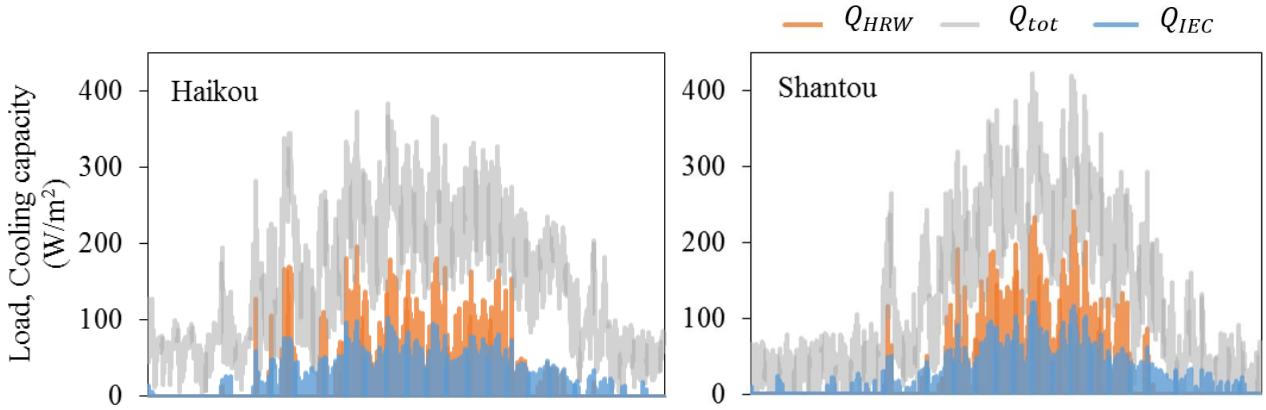

(a) Haikou (b) Shantou

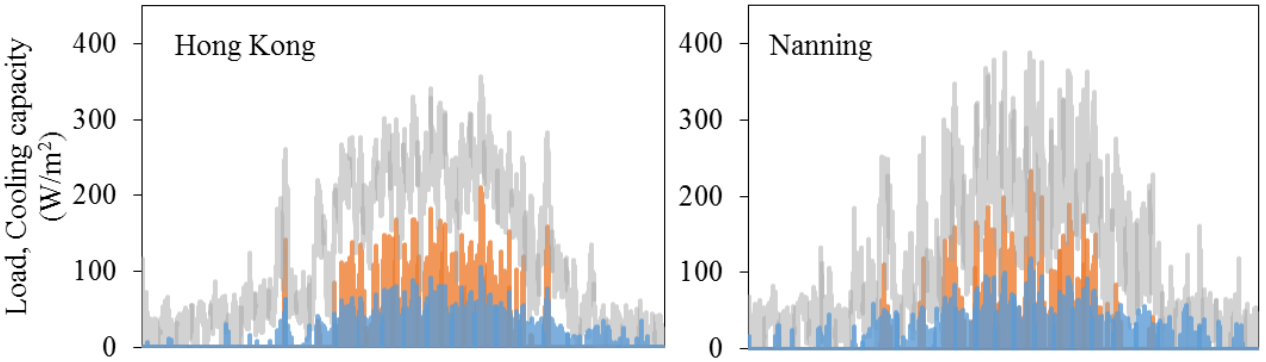

(c) Hong Kong (d) Nanning

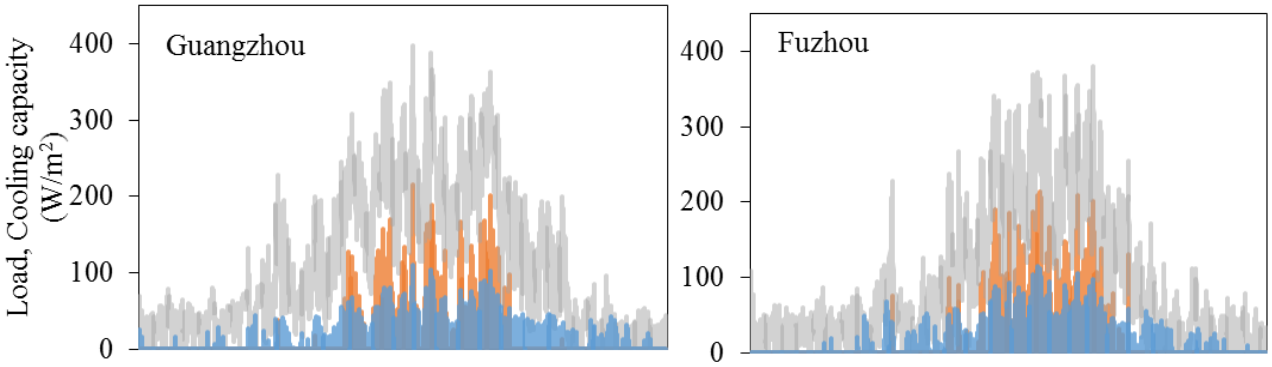

(e) Guangzhou (f) Fuzhou

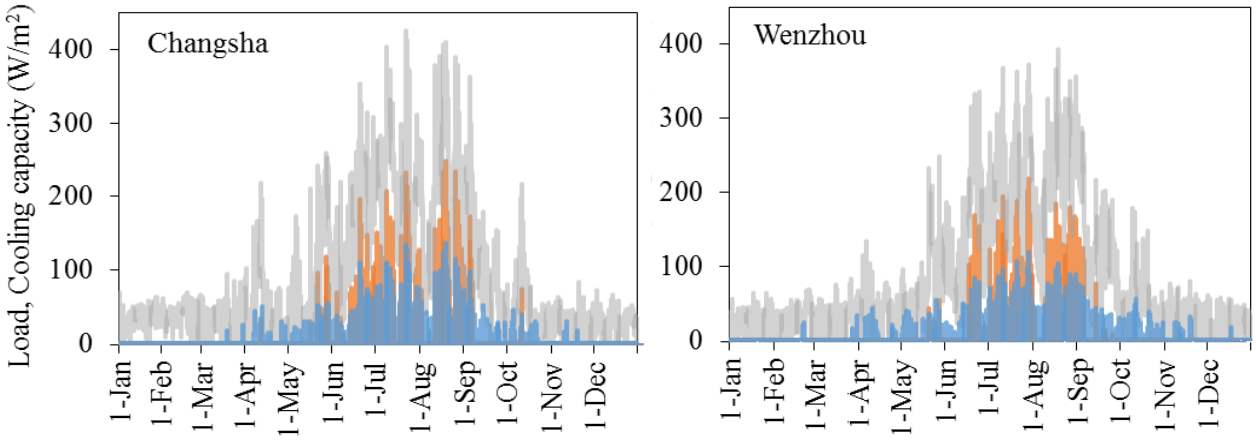

(g) Changsha (h) Wenzhou

Fig. 10. Cooling load handled by IEC and HRW in the studied wet market in 8 cities

For the wet market building, the size and configurations of the cooling systems will be determined based on the peak cooling load. Table 5 summarized the peak load reduction rate by using IEC and HRW respectively in the selected 8 cities. The cooling capacity provided by the IEC or HRW during the hour of the day in which the building has its maximum heat gain was used to calculate the peak load reduction rate of the two types of hybrid systems, respectively. Both two systems show great potentials in reducing the peak cooling load during summer periods, which not only cuts down the initial investment but also lessens the grid load. The AC+IEC system reduces the peak load for chillers by around 22.9–35.1% among these cities. The AC+HRW system provides higher peak load reduction in all of the selected cities, with a ratio of 44.5–48.1% under scenario A and 53.8-58.1% under scenario B. The larger peak cooling load reduction under scenario B (with indoor humidity control) can be attributed to the improved performance of IEC and HRW due to the drier exhaust air used for total heat recovery.

Table 5. Peak cooling load reduction using the two types of hybrid fresh air-handling systems in 8 cities

City	Annual cumulated building cooling load (MWh)	Peak cooling load (W/m^2)	Peak cooling load reduction			
			Scenario A		Scenario B	
			AC+IEC	AC+HRW	AC+IEC	AC+HRW
Haikou	699.4	382.4	30.8%	45.3%	34.1%	54.8%
Shantou	577.6	422.2	32.4%	48.1%	35.3%	56.3%
Hong Kong	549.1	357.1	22.9%	46.0%	28.0%	55.3%
Nanning	521.2	389.0	28.8%	47.4%	33.1%	57.2%
Guangzhou	512.2	397.6	29.3%	44.0%	35.1%	56.8%
Fuzhou	411.4	380.2	28.8%	46.0%	33.5%	56.8%

Changsha	406.0	425.4	31.5%	47.3%	35.7%	57.4%
Wenzhou	381.4	394.2	30.1%	44.5%	33.6%	53.8%

6.2 Cooling capacity

6.2.1 Sensible and latent cooling

Comparisons between the annual cumulated sensible and latent cooling capacity, as well as the cooling ratio of IEC and HRW in 8 different cities, were illustrated in Fig. 11. It is apparent that the IEC achieves a higher sensible cooling capacity than the HRW in all of the 8 selected cities, while the latent cooling capacity of HRW is always larger than that of the IEC. As shown in Fig. 11a, sensible cooling dominates in the total cooling capacity of IEC, accounting for 66.0–83.8% among these cities. By contrast, the total cooling capacity of HRW mainly attributes to the fresh air dehumidification, with a percentage of 53.4–61.1% for latent cooling in different cities. Under scenario A, the HRW has a higher total cooling ratio than the IEC in Haikou, Shantou, Hong Kong and Ningbo, while the IEC performs better than the HRW in the other cities, especially Fuzhou, Changsha and Wenzhou. Under scenario B, the cooling ratio achieved by the HRW is higher than that of IEC for all the cities. The two systems can undertake 20.2–36.7% of the annual cumulated total cooling load for decreasing the cooling coil capacity.

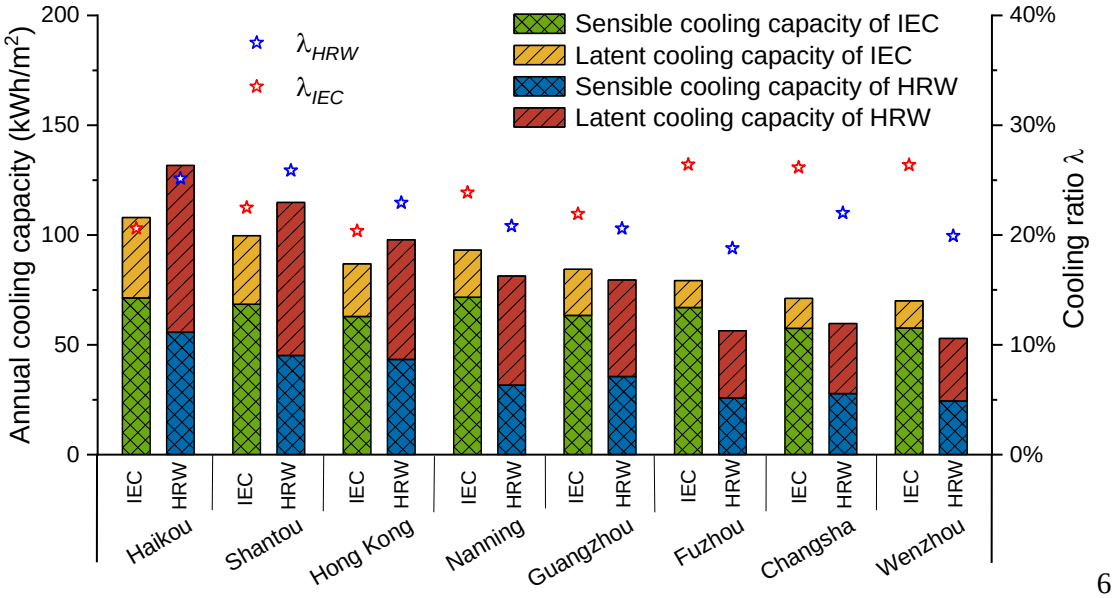

(a) Scenario A (without indoor humidity control)

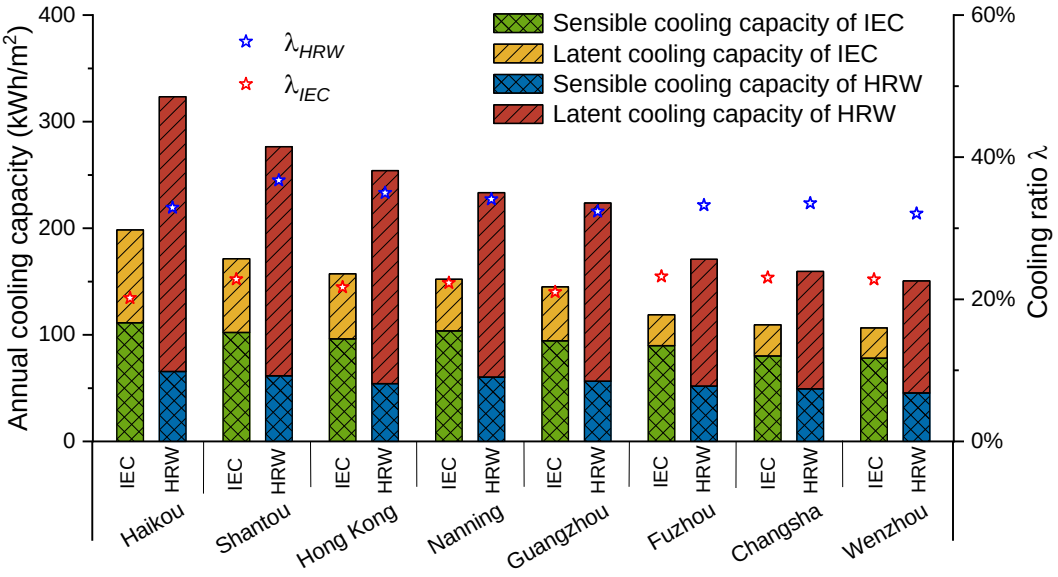

(b) Scenario B (with indoor humidity control)

Fig. 11 Annual cumulated sensible and latent cooling capacity, cooling ratio of IEC and HRW in 8 cities

Compared with scenario A, the annual total cooling capacity of the two systems is nearly doubled under scenario B. As the desired indoor relative humidity level is achieved under scenario B through overcooling and reheating the fresh air, the drier exhaust air is therefore produced, which greatly benefits the energy recovery performance. The effect of a lower exhaust air humidity ratio on the performance enhancement of HRW is more significant than of IEC. As shown in Fig. 11b, the annual latent cooling capacity of the HRW in Haikou has more than tripled from 76.0 kWh/m^2 to 257.8 kWh/m^2.

6.2.2 Total cooling performance

Fig. 12 compares the cumulated total cooling capacity of IEC and HRW in the selected 8 cities. The *x*-axis indicates the annual average relative humidity of the ambient air in different cities. The *y*-axis represents the differences between the cooling capacity of HRW and IEC ($Q_{HRW} - Q_{IEC}$). Among these cities, the annual average ambient temperature varied from 18.1°C in Changsha to 23.7°C in Haikou, and the annual average ambient relative humidity varied from 72% in Wenzhou to 85% in Haikou.

It is observed that the differences between the cooling capacity of IEC and HRW show a close correlation with the local ambient relative humidity. In Fig. 12a, it is suggested that the correlated linear equation can provide references for comparing the applicability of the IEC and HRW in a building under scenario A. If the local annual average relative humidity of ambient air is lower than 76%, the IEC is more applicable as it handles more cooling load than the HRW. In Fig. 12b, it is clarified that the HRW has prominent

superiority over the IEC under scenario B in all the selected cities. The more humid local weather conditions can result in greater differences between the HRW and IEC on the total cooling capacity.

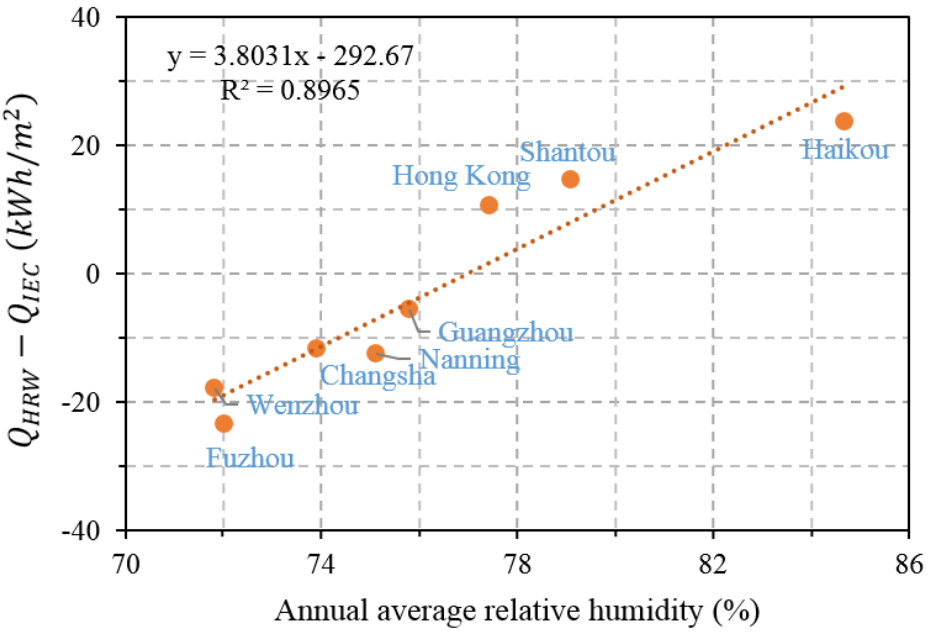

(a) Scenario A: without indoor humidity control

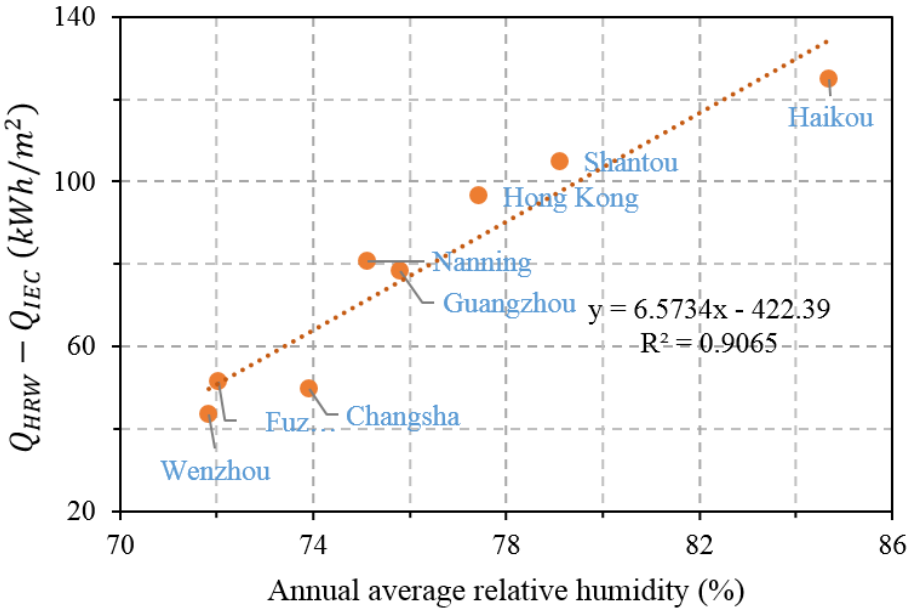

(b) Scenario B: with indoor humidity control

Fig. 12 Differences between the annual cumulated total cooling capacity of IEC and HRW versus the annual average ambient relative humidity of 8 cities

6.3 Energy efficiency

Fig. 13 shows the annual energy intensity of the two types of hybrid fresh air-handling systems in the selected 8 cities. The energy demand of the stand-alone AHU unit that handles all the cooling load was used as a baseline to analyze the energy consumption of the AC+IEC and AC+HRW system, respectively. Under scenario A, the highest energy saving intensity of the AC+IEC (95.7 MJ/m^2) and AC+HRW (109.6 MJ/m^2) are both achieved in Haikou due to its extremely hot and humid climate. The lowest energy-saving intensity is achieved in Wenzhou of 64.2 MJ/m^2 for the AC+IEC and 45.5 MJ/m^2 for the AC+HRW. It is found in Fig. 13a that the annual energy consumption intensity of the HRW (ranges in 11.2–26.5 MJ/m^2) is higher than that of the IEC (ranges in 8.5–15.4 MJ/m^2) in all the selected cities. Due to the small air pressure drop, the IEC consumes less energy to cool the fresh air, even if its annual feasible operating period is longer than that of the HRW. Taking Hong Kong as an example, although the HRW handles more cooling load and the power consumed by AC is lower, the AC+IEC system can still be competitive in these cities due to the very close total energy consumption intensity.

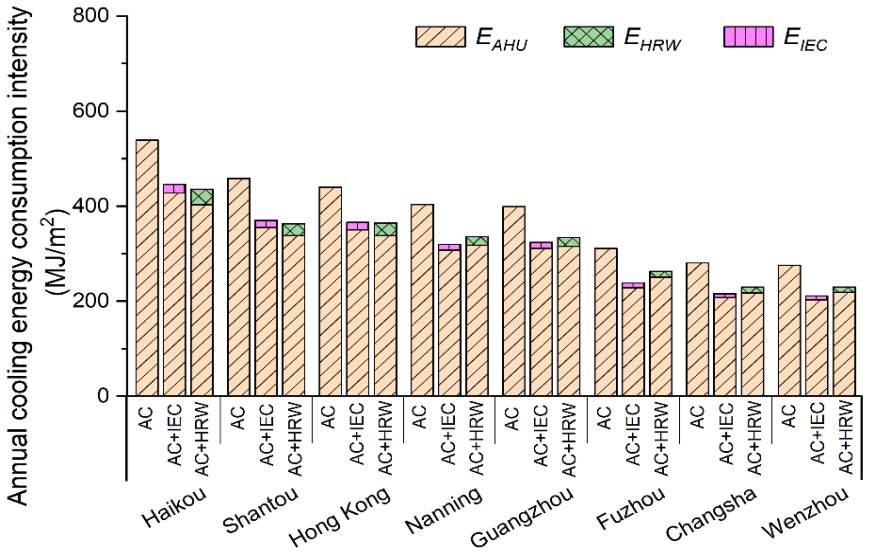

(a) Scenario A (without indoor humidity control)

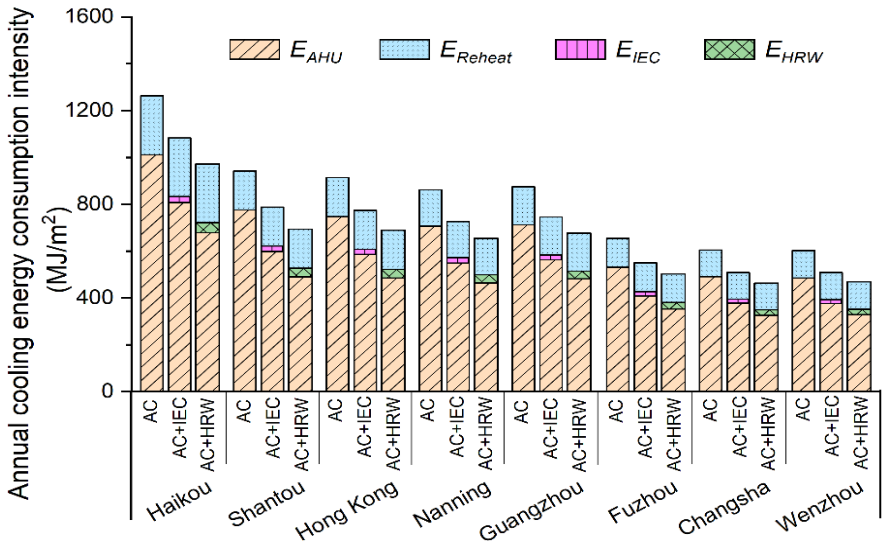

(b) Scenario B (with indoor humidity control)

Fig. 13 Annual cooling energy consumption intensity of AC+IEC and AC+HRW system compared with baseline AC system in 8 cities

Fig. 13b presents the annual energy consumption intensity of the AC systems with indoor humidity control. It can be seen that the energy required for reheating accounts for a significant fraction (17.6–20.4%) of the total cooling energy requirement in these cities. The difference between the energy demands of the baseline system and the two types of hybrid systems is the energy consumption of air-handling unit, which is greatly saved in both two systems. The energy-saving intensity of the two systems under scenario B is higher than those under scenario A. Specifically, the energy-saving intensity of the AC+HRW system (125.8–295.8 MJ/m^2) outweighs a lot than that of the AC+IEC system (80.4–181.8 MJ/m^2). Therefore, employing the AC+HRW system is more suitable for buildings with indoor humidity-controlled due to the higher efficiency of fresh air dehumidification.

The energy-saving ratios of the two types of hybrid systems operated under scenarios A and B are indicated in Fig. 14. Among the selected 8 cities with hot and humid climates, the energy-saving ratios of the two systems range from 14.4% to 26.4%. Under scenario A, the maximum energy saving ratios are attained by AC+IEC system in the cities with moderate humid subtropical climatic, namely Fuzhou (23.4%), Wenzhou (23.3%) and Changsha (23.1%). However, the AC+HRW system is more energy-efficient when operates under scenario B. The AC+HRW system can achieve 22.2–26.4% of energy savings for the buildings with indoor humidity-controlled among these selected cities.

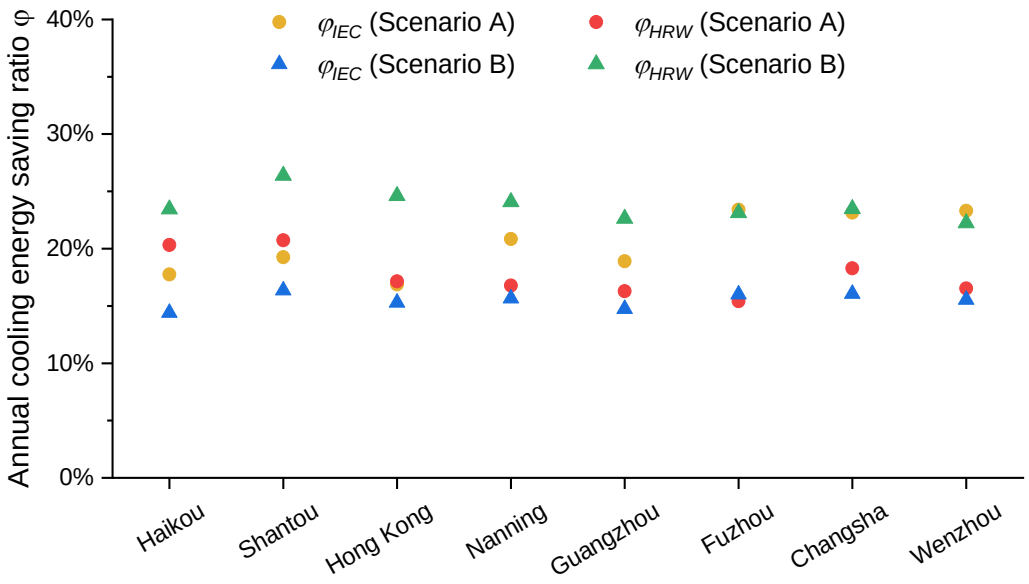

Fig. 14 Annual cooling energy saving ratios by IEC and HRW in 8 cities

7. Conclusions

In this study, the applicability of indirect evaporative cooler (IEC) for exhaust air energy recovery in the central air-conditioning (AC) systems in hot and humid areas was quantitatively addressed and compared to a traditional hybrid AC system integrated with a heat recovery wheel (HRW). A field-based investigation was carried out in a wet market located in Hong Kong, and the annual building energy simulation was conducted by incorporating the mathematical models into TRNSYS platform for assessing the performance of two systems in different cities. The main conclusions are as follows.

(1) The operation data of the two systems during a typical summer day indicates that the IEC has better sensible cooling performance, with an average outlet air temperature difference of 4.0°C lower than the HRW. In contrast, the HRW achieves a greater dehumidifying effect, as the average outlet air humidity ratio was 3.2g/kg lower than that of the IEC.

(2) From the annual simulation results, the HRW achieves higher peak cooling load reduction (44.5–58.1%) for the AC system than the IEC (22.9–35.1%) during summer times in 8 selected cities. However, the IEC has a longer feasible operating period than the HRW under moderate temperature and humidity conditions, as it utilizes the exhaust air with water evaporation. The two energy recovery units can handle 20.2–36.7% of the annual cumulated total cooling load for the central AC system.

(3) The sensible cooling of the IEC accounts for 66–84% of total cooling capacity among these cities, while the latent cooling dominates (53–61%) in the HRW. The total cooling capacity differences between the IEC and HRW showed a nearly linear relationship with the local ambient relative humidity. In cities

where the annual average relative humidity of ambient air is lower than 76%, the IEC provides a larger cooling capacity than the HRW.

(4) Under the scenario without indoor humidity control, the energy-saving intensity of the AC+IEC system (64.2–73.4 MJ/m^2) outweighs that of the AC+HRW system (45.5–51.8 MJ/m^2) in some cities (Fuzhou, Wenzhou and Changsha). Under the scenario with indoor humidity control, the total cooling capacity of HRW overtakes that of the IEC by 28.9–38.6% among all the selected cities. The reduction in exhaust air relative humidity could significantly enhance the cooling performance of the HRW.

(5) Annual energy-saving ratios of the two types of hybrid systems range from 14.4% to 26.4%. The AC+IEC is more energy-efficient for the buildings without humidity control under the moderate humid subtropical climatic, such as Fuzhou, Wenzhou and Changsha. The AC+HRW system is more applicable for the buildings with indoor humidity controlled, and especially suitable for cities with a perennially humid climate, such as Haikou, Shantou and Hong Kong.

Appendix A

Table A1. Values of main parameters in the HRW model

Symbol	Parameter	Unit	Value
a	pore radius of the desiccant	-	1.5×10^{-9} [42]
C	shape factor of desiccant material	-	1.1
c_{pd}	specific heat of dry desiccant	kJ kg^{-1} K^{-1}	0.92
c_{pg}	specific heat of substrate	kJ kg^{-1} K^{-1}	0.88
c_{pw}	specific heat of water	kJ kg^{-1} K^{-1}	4.18
D_0	constant for surface diffusion calculation	-	1.6×10^{-6} [42]
d_e	hydrodynamic diameter of the channel	m	1.2×10^{-3}
f	volume ratio of the desiccant material in the solid	-	0.7 [21]
Le	Lewis number	-	1
M_1	the molecule weight of water	kg kmol^{-1}	18
Nu	Nusselt number	-	2.46 [43]
P_a	atmosphere pressure	Pa	101325
q_{st}	adsorption heat	kJ kg^{-1}	2380
w_{max}	maximum water content of the desiccant	kg kg^{-1}	0.35
ρ_d	density of desiccant wall	kg/m^3	770
ζ	tortuosity factor of the channel	-	2.8 [42]
ε_t	total porosity	-	0.56 [44]
λ_d	thermal conductivity of desiccant	kW m^{-1} K^{-1}	1.74×10^{-4}

In Eq. (9), the total specific heat capacity of the wet desiccant wall (c_{tot}) is influenced by the equilibrium water content of the desiccant (w), as shown in Eq. (A.1).

$$c_{tot} = f\left(c_{pd} + wc_{pw}\right) + (1-f)c_{pg} \tag{A.1}$$

The iso-water content line of the desiccant will coincide with the iso-relative humidity line of the humid air. A general sorption isotherm is widely used to govern the w, as expressed in Eq. (A.2).

$$w = \frac{w_{max}}{1 - C + C/\phi} \tag{A.2}$$

where, ϕ is relative humidity of the moist air. The relationship between relative humidity and moisture content (ω) of moist air can be described using Clapeyron equation, as shown in Eq. (A.3).

$$\frac{\phi}{\omega} = 10^{-6}e^{5294/T_a} - 1.61\phi \tag{A.3}$$

The gas diffusion (D_A) and surface diffusion (D_S) are calculated by Eqs. (A.4) and (A.5) [45], respectively.

$$D_A = \frac{\varepsilon_t}{\zeta}\left(\frac{1}{D_{AO}} + \frac{1}{D_{AK}}\right)^{-1}, where\ D_{AO} = 1.758\times10^{-4}\frac{T_d^{1.685}}{P_a}, \qquad D_{AK} = 97a\left(\frac{T_d}{M_1}\right)^{0.5} \tag{A.4}$$

$$D_S = \frac{1}{\zeta}D_0 exp\left(\frac{-0.974\times10^{-3}q_{st}}{T_d}\right) \tag{A.5}$$

where, D_{AO} is the ordinary diffusivity and D_{AK} is the Knudsen diffusivity.

Table A2. Values of main parameters in the IEC model

Symbol	Parameter	Unit	Value
d_e	hydrodynamic diameter of the channel	m	8.0×10^{-3}
Le	Lewis number	-	1
Nu	Nusselt number		8.235 [46]
Pr	Prandlt number	-	0.7
λ_a	thermal conductivity of air	kW m^{-1} K^{-1}	3.0×10^{-5}

The convective heat transfer coefficient (h) can be calculated by Eq. (A.6).

$$Nu = \frac{\mathrm{h}d_e}{\lambda_a} \tag{A.6}$$

For the moist air flow in wet channels, the relationship between heat and mass transfer coefficients can be expressed by Eq. (A.7).

$$h_m = \frac{\mathrm{h}}{c_{pa}Le} \tag{A.7}$$

The boundary conditions for the governing equations of IEC are:

$$\begin{cases} t_p(x=0) = t_{p,in},\ \omega_p(x=0) = \omega_{p,in} \\ m_c(x=0) = 0 \\ t_s(y=0) = t_{s,in},\ \omega_s(y=0) = \omega_{s,in} \\ m_e(y=1) = m_{e,in} \end{cases}$$

CRediT authorship contribution statement

Yunran Min: Conceptualization, Methodology, Software, Data curation, Writing original draft. Yi Chen: Investigation, Writing review & editing. Wenchao Shi: Investigation, Writing review & editing. Hongxing Yang: Supervision, Project administration, Funding acquisition.

Acknowledgment

The work described in this paper was financially supported by the GRF research projects (No.: Q73F and Q78C) of the Research Grants Committee, the Hong Kong SAR Government. Supports from the Research Institute for Sustainable Urban Development of The Hong Kong Polytechnic University is appreciated.

References:

[1] Zhang L-Z, Zelik EB. Total heat recovery: heat and moisture recovery from ventilation air: Nova Science Publ.; 2008.
[2] Hu M, Xiao F, Jørgensen JB, Wang S. Frequency control of air conditioners in response to real-time dynamic electricity prices in smart grids. Applied Energy. 2019;242:92-106.
[3] National Bereau of Statistics of the People's Republic of China, National Bereau of Statistics of the People's Republic of China, 2017, China Energy Statistical Yearbook, China Statistics Press, Beijing (2017).
[4] Zhuang C, Wang S, Shan K. Probabilistic optimal design of cleanroom air-conditioning systems facilitating optimal ventilation control under uncertainties. Applied Energy. 2019;253:113576.
[5] Chua KJ, Chou SK, Yang WM, Yan J. Achieving better energy-efficient air conditioning – A review of technologies and strategies. Applied Energy. 2013;104:87-104.
[6] Lyu W, Li X, Wang B, Shi W. Energy saving potential of fresh air pre-handling system using shallow geothermal energy. Energy and Buildings. 2019;185:39-48.
[7] Liu J, Li W, Liu J, Wang B. Efficiency of energy recovery ventilator with various weathers and its energy saving performance in a residential apartment. Energy and Buildings. 2010;42:43-9.
[8] Zhong K, Kang Y. Applicability of air-to-air heat recovery ventilators in China. Applied Thermal Engineering. 2009;29:830-40.
[9] Lee S, Lee W. Site verification and modeling of desiccant-based system as an alternative to conventional air-conditioning systems for wet markets. Energy. 2013;55:1076-83.
[10] Chen L, Chen S, Liu L, Zhang B. Experimental investigation of precooling desiccant-wheel air-conditioning system in a high-temperature and high-humidity environment. International Journal of Refrigeration. 2018;95:83-92.
[11] Yamaguchi S, Saito K. Numerical and experimental performance analysis of rotary desiccant wheels. International Journal of Heat and Mass Transfer. 2013;60:51-60.
[12] Rey Martínez FJ, Velasco Gómez E, Martín García C, Sanz Requena JF, Navas Gracia LM, Hernández Navarro S, et al. Life cycle assessment of a semi-indirect ceramic evaporative cooler vs. a heat pump in two climate areas of Spain. Applied Energy. 2011;88:914-21.
[13] Labban O, Chen T, Ghoniem AF, Lienhard JH, Norford LK. Next-generation HVAC: Prospects for and limitations of desiccant and membrane-based dehumidification and cooling. Applied Energy. 2017;200:330-46.
[14] Karami M, Delfani S, Noroozi A. Performance characteristics of a solar desiccant/M-cycle air-conditioning system for the buildings in hot and humid areas. Asian Journal of Civil Engineering. 2019:1-11.
[15] Lin J, Wang RZ, Kumja M, Bui TD, Chua KJ. Modelling and experimental investigation of the cross-flow dew point evaporative cooler with and without dehumidification. Applied Thermal Engineering. 2017;121:1-13.
[16] Cui X, Chua K, Yang W, Ng K, Thu K, Nguyen VJATE. Studying the performance of an improved dew-point evaporative design for cooling application. 2014;63:624-33.
[17] Zanchini E, Naldi C. Energy saving obtainable by applying a commercially available M-cycle evaporative cooling system to the air conditioning of an office building in North Italy. Energy. 2019;179:975-88.
[18] Cui X, Chua K, Islam M, Yang W. Fundamental formulation of a modified LMTD method to study indirect evaporative heat exchangers. Energy conversion and management. 2014;88:372-81.
[19] Cui X, Mohan B, Islam M, Chua K. Investigating the energy performance of an air treatment incorporated cooling system for hot and humid climate. Energy and Buildings. 2017;151:217-27.
[20] Angrisani G, Minichiello F, Roselli C, Sasso M. Experimental analysis on the dehumidification and thermal performance of a desiccant wheel. Applied Energy. 2012;92:563-72.
[21] Tu R, Liu X-H, Jiang Y. Performance comparison between enthalpy recovery wheels and dehumidification wheels. International Journal of Refrigeration. 2013;36:2308-22.

[22] Kim H-J, Ham S-W, Yoon D-S, Jeong J-W. Cooling performance measurement of two cross-flow indirect evaporative coolers in general and regenerative operation modes. Applied Energy. 2017;195:268-77.
[23] Zheng B, Guo C, Chen T, Shi Q, Lv J, You Y. Development of an experimental validated model of cross-flow indirect evaporative cooler with condensation. Applied Energy. 2019;252:113438.
[24] Min Y, Chen Y, Yang H. A statistical modeling approach on the performance prediction of indirect evaporative cooling energy recovery systems. Applied Energy. 2019;255:113832.
[25] Min Y, Chen Y, Yang H, Guo C. Characteristics of primary air condensation in indirect evaporative cooler: Theoretical analysis and visualized validation. Building and Environment. 2020:106783.
[26] Comino F, de Adana MR, Peci F. Energy saving potential of a hybrid HVAC system with a desiccant wheel activated at low temperatures and an indirect evaporative cooler in handling air in buildings with high latent loads. Applied Thermal Engineering. 2018;131:412-27.
[27] Climate of Hong Kong (1981-2010), Hong Kong Observatory, Available at: https://www.hko.gov.hk/en/cis/climahk.htm; 2020.
[28] Chen Y, Yang H, Luo Y. Parameter sensitivity analysis and configuration optimization of indirect evaporative cooler (IEC) considering condensation. Applied Energy. 2017;194:440-53.
[29] Fu H, Liu X, Xie Y, Jiang Y. Experimental and numerical analysis on total heat recovery performance of an enthalpy wheel under high temperature high humidity working conditions. Applied Thermal Engineering. 2019;146:482-94.
[30] Fu H-X, Zhang L-Z, Xu J-C, Cai R-R. A dual-scale analysis of a desiccant wheel with a novel organic–inorganic hybrid adsorbent for energy recovery. Applied energy. 2016;163:167-79.
[31] Min Y, Chen Y, Yang H. Numerical study on indirect evaporative coolers considering condensation: A thorough comparison between cross flow and counter flow. International Journal of Heat and Mass Transfer. 2019;131:472-86.
[32] MOHURD. Code for Design of Civil Buildings. Ministry of housing and Urban-Rural development of the people's Republic of China (2005).
[33] Administration CM. China meteorological data service center, https://data.cma.cn/data/weatherBk.html. Access: Augest 2020.
[34] Refrigerating ASoH, Air-Conditioning. 2017 ASHRAE handbook: Fundamentals (SI). American Society of Heating Refrigerating and Air-Conditioning Atlanta; 2017.
[35] Klein S. et al. TRNSYS 17: a transient system simulation program, 2010. Solar Energy Laboratory, University of Wisconsin, Madison, USA.
[36] Lee WL, Chen H, Leung YC, Zhang Y. Decoupling dehumidification and cooling for energy saving and desirable space air conditions in hot and humid Hong Kong. Energy Conversion and Management. 2012;53:230-9.
[37] Zhuang C, Wang S, Shan K. Adaptive full-range decoupled ventilation strategy and air-conditioning systems for cleanrooms and buildings requiring strict humidity control and their performance evaluation. Energy. 2019;168:883-96.
[38] Cui X, Chua K, Islam M, Ng K. Performance evaluation of an indirect pre-cooling evaporative heat exchanger operating in hot and humid climate. Energy conversion and management. 2015;102:140-50.
[39] Chen C-H, Hsu C-Y, Chen C-C, Chiang Y-C, Chen S-L. Silica gel/polymer composite desiccant wheel combined with heat pump for air-conditioning systems. Energy. 2016;94:87-99.
[40] You T, Yang H. Feasibility of ground source heat pump using spiral coil energy piles with seepage for hotels in cold regions. Energy Conversion and Management. 2020;205:112466.
[41] Guideline A. Guideline 14-2002. Measurement of energy and demand savings. 2002;22.
[42] Zhang L, Niu J. Performance comparisons of desiccant wheels for air dehumidification and enthalpy recovery. Applied Thermal Engineering. 2002;22:1347-67.
[43] Shah RK, London AL. Laminar flow forced convection in ducts: a source book for compact heat exchanger analytical data: Academic press. ; 2014.
[44] Ng K, Chua H, Chung C, Loke C, Kashiwagi T, Akisawa A, et al. Experimental investigation of the silica gel–water adsorption isotherm characteristics. Applied Thermal Engineering. 2001;21:1631-42.

[45] Pesaran AA, Mills AF. Moisture transport in silica gel packed beds—I.Theoretical study. International Journal of Heat and Mass Transfer. 1987;30:1037-49.
[46] Riangvilaikul B, Kumar S. Numerical study of a novel dew point evaporative cooling system. Energy and Buildings. 2010;42:2241-50.